Peristaltic Transport of Couple Stress Fluid through an Inclined Asymmetric and Non- Uniform Channel with Porous Medium

Hanaa Abdulhussain[1], Ahmed M. Abdulhadi[2]

[1, 2]University of Baghdad, Department of Mathematic, Baghdad, Iraq

Abstract: *This paper investigated the effect of channel inclination on the peristaltic transport of a couple stress fluid in an asymmetric and non-uniform channel through the porous medium under the action of an externally applied magnetic field .The effects of slip velocity on the channel walls have been taken into account and the effects particle size . The non-linearity of the problem is analyzed by using the long wave length and low Reynolds number approximations. The mathematical expressions for axial velocity, stream function, pressure gradient and pressure rise per wave length have been derived analytically. The above said quantities are computed for a specific set of values of the different Parameters involved in the present model .The computational results are presented in the form of graphs . It is observed that, pressure gradient increases with the increase of Hartmann number , Froude number whereas it decreases with the increasing values of the inclination angle of the channel, Darcy number, slip parameter, couple stress parameter and Reynolds number as well as non-uniform parameter of the channel. This study puts an important observation that the occurrence of trapping bolus can be eliminated with suitably adjusting couple stress effect and the application of strong magnetic field . The role of slip velocity has a reducing effect on the bolus size. Moreover, The size of the bolus is increased by increasing the Darcy number and non-uniform parameter of the channel.*

Keywords: Couple stress fluid, slip velocity, peristaltic flow, non-uniform channel, porous medium,an inclined asymmetric channel

1. Introduction

It is well known that mixing and transporting of physiological fluids is referred as peristalsis, which is generated due to progressive waves of area contraction and expansion along the length of a distensible tube containing fluid. The mechanism behind this phenomenon is mainly neuromuscular property of any tubular smooth muscle structure. This type of muscular tube wall has a motion in wave frame with a fixed speed and wave length. This mechanism is found in urine transport from kidney to the bladder, the movement of chime into the gastrointestinal tract, fluids in the lymphatic vessels, bile from the gallbladder into the duodenum, the movement of spermatozoa in the ducts efferent of the male reproductive tract, the movement of the ovum in the fallopian tube and the circulation of blood in small blood vessels. This mechanism also finds many applications in bio-medical engineering to design roller and finger pumps, some bio-mechanical instruments, e.g., heart- lung machine, blood pump machine and dialysis machine. Akbar el at.[1] Peristaltic flow of a Williamson fluid in an inclined asymmetric channel with partial slip and heat transfer .Ali and Hayat[2] they have studied on the peristaltic flow of a micropolar fluid in an asymmetric channel by considering different kind of fluid models, wherein they found distinguishable effect of phase difference of wall motion on velocity and other flow characteristics. Kothandapani and Srinivas [3] have considered the non-linear peristaltic transport of a Newtonian fluid in an inclined asymmetric channel through a porous medium. However, to the best of author's knowledge, no one has considered the slip effect on peristaltic transport of couple stress fluid in an inclined asymmetric channel along with the externally applied magnetic field. Mekheimer[4] Effect of induced magnetic field on peristaltic flow of a couple stress fluid. Mishra and Rao [5] Peristaltic transport

of a Newtonian fluid in an asymmetric channel. Ramesh [6] Influence of heat and mass transfer on peristaltic flow of a couple stress fluid through porous medium in the presence of inclined magnetic field in an inclined asymmetric channel. The idea of pumping characteristics was first introduced by Shapiro et al. [7] that the pumping is determined through the variation in time averaged flux with difference in pressure across one wave length. It is well known that, if the flow is steady in the wave frame the instantaneous pressure difference between two stations of one wave length apart is a constant. Shit and Ranjit [8] investigation of peristaltic transport of a couple stress fluid in an asymmetric and non-uniform channel under the action of an externally applied magnetic field. Shit and Roy [9] Hydromagnetic effect on inclined peristaltic flow of a couple stress fluid. Therefore, our motivation is to examine the role of boundary slip when the non-uniform channel walls contracting and expanding. Srinivas and Pushparaj [10] Non- linear peristaltic transport in an inclined asymmetric channel. The couple-stress fluid may be considered as a special class of a non-Newtonian fluid, which takes into account the effect of particle size. To characterize the couple stress fluid, Stokes [11] gave a concept of constitutive relationship between the stress and strain rate in micro-continuum theory of fluids which allows for polar effects such as the presence of couple stresses, body couples and a non-symmetric stress tensor. The constitutive equations in these fluid models are very complex because of the involvement of various material constants leading to a boundary value problem so that the order of the differential equations is higher than the Navier-Stokes equations. He found that pressure rise is greater for a couple stress fluid than a Newtonian fluid model under similar circumstances. Owing to the abovementioned studies, we have investigated the effect of slip velocity on peristaltic flow of a couple stress fluid through an inclined asymmetric and non-uniform channel with porous medium . The long wave length and low

Reynolds number assumptions have been made to simplify the highly nonlinear terms in the governing equations. Therefore, our theoretical investigation bears the potential to useful in the field of bio-fluid dynamics.

2. Mathematical Formulation and Solution

Consider the peristaltic transport of an incompressible couple-stress fluid through an inclined asymmetric and non-uniform channel with porous medium under the action of an external magnetic field. generated by propagation of waves on the channel walls travelling with different amplitudes and phases but with constant speed c (see Fig.1).
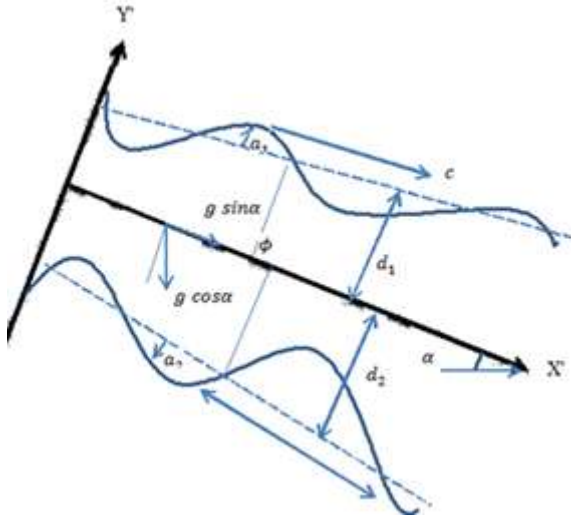
Figure 1: A physical sketch of the problem

Let $Y' = h_1'$ (X',t') and $Y' = h_2'$ (X',t') represent respectively the upper wall and lower wall of the channel ,such that

$$h_1' (X',t') = d_1 + (X' - ct') \tan\alpha + a_1 \cos\left[\frac{2\pi}{\lambda}(X' - ct')\right] \quad (1)$$

$$h_2' (X',t') = -d_2 - (X' - ct') \tan\alpha + a_2 \cos\left[\frac{2\pi}{\lambda}(X' - ct' + \phi)\right] (2)$$

where a_1 and a_2 are the amplitudes of waves, λ is the wave length, ϕ $(0 \leq \phi \leq \pi)$ the phase difference between the channel walls . X' and Y' are the rectangular Cartesian co-ordinates with X' measures the axis of the channel and Y' the transverse axis perpendicular to X'. d_1 and d_2 are the constant height of the upper wall and lower wall of the channel from the central line and α denotes the inclination of the channel walls with the central axis- X'.The system is stressed by an external transverse uniform constant magnetic field of strength B_o. Due to the imposition of an external magnetic field in an electrically conducting fluid, there arises electromotive force (emf) inducing a current inside the flow region. Since the electrical conductivity of liquid is very small, the magnetic Reynolds number becomes too small. Therefore, we have neglected the induced electrical filed as well as induced magnetic field.

The equations of motion for unsteady flow through an asymmetric channel of an incompressible couple stress fluid(cf. [3], [11])with externally imposed magnetic field by neglecting the body couples are ,

$$\vec{\nabla}.\vec{V'} = 0 \quad (3)$$

$$\rho\left(\frac{\partial \vec{V'}}{\partial t'} + (\vec{V'}.\vec{\nabla})\vec{V'}\right) = -\vec{\nabla}P' + \mu\nabla^2\vec{V'} - \eta\nabla^4\vec{V'} + \vec{j'} \times \vec{B'} - \frac{\mu}{k_\circ}\vec{V'} + \rho g(i\sin\alpha - j\cos\alpha)(4)$$

$$\rho\left(\frac{\partial u'}{\partial t'} + U'\frac{\partial u'}{\partial x'} + V'\frac{\partial u'}{\partial y'}\right)$$
$$= -\frac{\partial P'}{\partial x'} + \mu\nabla^2 u' - \eta\nabla^4 u' + (J' \times B')_x$$
$$- \frac{\mu}{k_o}u' + \rho g \sin\alpha \quad (5)$$

$$\rho\left(\frac{\partial v'}{\partial t'} + U'\frac{\partial v'}{\partial x'} + V'\frac{\partial v'}{\partial y'}\right) = -\frac{\partial P'}{\partial y'} + \mu\nabla^2 v' - \eta\nabla^4 v'$$
$$+ (J' \times B')_y - \frac{\mu}{k_o}v' - \rho g \cos\alpha \quad (6)$$

where $\vec{V'} = (U', V', 0)$ be the velocity vector, P' is the fluid pressure, ρ the fluid density, μ the dynamic viscosity of the fluid, η is the constant associated with couple stress effect, $\vec{B}$ $(0, B_o , 0)$ the magnetic field vector, $\vec{E}$ the electric field vector, g be the acceleration due to gravity , σ denotes the electrical conductivity of the fluid and $\vec{j}$ is the current vector due to Ohm's law, given by $\vec{j'} = \sigma(\vec{E'} + \vec{V'} \times \vec{B'})$. fourth term on the right hand side of Eq.(4) represent the body force per unit volume due to the application of an external magnetic field. Due to the assumption of low magnetic Reynolds number, the induced electric field is neglected. Therefore, the Ohm's law simply reduces to $\vec{j'} = \sigma(\vec{V'} \times \vec{B'})$ It is noted that in our model there is no external electric field.

and $\nabla^2 = \frac{\partial^2}{\partial x'^2} + \frac{\partial^2}{\partial y'^2}$

, $\nabla^4 = \frac{\partial^4}{\partial x'^4} + 2\frac{\partial^4}{\partial x'^2 y'^2} + \frac{\partial^4}{\partial y'^4}$.

It is further noticed that the flow field in laboratory frame (X', Y') and wave frame (x ',y') are treated as unsteady and steady motion respectively. Considering the relation between the wave frame (x', y') moving with a velocity c away from a fixed frame (X', Y') that follows from the following transformations.In addition to equation (5) and (6)become

$$\frac{\partial u'}{\partial t'} = 0 , \frac{\partial v'}{\partial t'} = 0$$

$$v'(x',y') = V' \quad ,y' = Y', \quad x' = X' - ct', U' = u' (x',y')$$

In which (u', v') and (U',V') are respectively the velocity components in the wave and laboratory frames. Using the abovementioned transformations, the governing Eqs .(3) ,(5)and (6) can be written in the wave frame of reference as .

$$\frac{\partial u'}{\partial x'} + \frac{\partial v'}{\partial y'} = 0 \quad (7)$$

$$\rho\left((u' + c)\frac{\partial u'}{\partial x'} + v'\frac{\partial u'}{\partial y'}\right) = -\frac{\partial P'}{\partial x'} + \mu\nabla^2 u' - \eta\nabla^4 u'$$
$$+ \sigma B_o^2(u' + c) - \frac{\mu}{k_o}u' + \rho g \sin\alpha \quad (8)$$

$$\rho\left((u' + c)\frac{\partial v'}{\partial x'} + v'\frac{\partial v'}{\partial y'}\right) = -\frac{\partial P'}{\partial y'} + \mu\nabla^2 v' - \eta\nabla^4 v'$$
$$- \frac{\mu}{k_o}v' - \rho g \cos\alpha \quad (9)$$

Let us introduce the following non-dimensional variables (cf. Mishra and Rao[5]).

$P,,t = \frac{ct'}{\lambda}\psi = \frac{\psi'}{cd_1} = \ , \ y = \frac{y'}{d_1} \ , \ x = \frac{x'}{\lambda}, \omega = \frac{\omega' d_1}{c}, \frac{d_1^2 P'(X)}{\lambda \mu c}$

$u = \frac{u'}{c}, v = \frac{\lambda v'}{cd_1}$

$h_1(x) = \frac{h_1'(x)}{d_1} = 1 + \left(\frac{\lambda \tan \alpha}{d_1}\right)x + \frac{a_1}{d_1}\cos(2\pi x)$ (10)

$h_2(x) = \frac{h_2'(x)}{d_1} = -\frac{d_2}{d_1} - \left(\frac{\lambda \tan \alpha}{d_1}\right)x + \frac{a_1}{d_1}\cos(2\pi x + \phi)$ (11)

where ψ represents the dimensionless stream function in which the velocity components u and v given by $u = \frac{\partial \psi}{\partial y}$ and $v = -\frac{\partial \psi}{\partial x}$ satisrying the continuity Eq. (7).

Using the non-dimensional variables defined in Eqs. (8), (9), (10) and (11) transformed into following equations in terms of stream function ψ as

$Re.\delta\left[\left(\frac{\partial \psi}{\partial y}.\frac{\partial}{\partial x} - \frac{\partial \psi}{\partial x}.\frac{\partial}{\partial y}\right)\frac{\partial \psi}{\partial y} + \frac{\partial^2 \psi}{\partial x \partial y}\right] = -\frac{\partial P}{\partial x} + \delta^2\frac{\partial^3 \psi}{\partial x^2 \partial y}$

$+ \frac{\partial^3 \psi}{\partial y^3} - \frac{1}{\gamma^2}\left(\delta^4\frac{\partial^5 \psi}{\partial x^4 \partial y} + 2\delta^2\frac{\partial^5 \psi}{\partial x^2 \partial y^3} + \frac{\partial^5 \psi}{\partial y^5}\right)$

$-H_a^2\left(\frac{\partial \psi}{\partial y} + 1\right) - \frac{1}{Da}.\frac{\partial \psi}{\partial y}$
$+ \frac{Re}{Fr}\sin[\alpha]$ (12)

$Re.\delta^3\left[\left(-\frac{\partial \psi}{\partial y}.\frac{\partial}{\partial x} + \frac{\partial \psi}{\partial x}.\frac{\partial}{\partial y}\right)\frac{\partial \psi}{\partial x} - \frac{\partial^2 \psi}{\partial x^2}\right] = -\frac{\partial P}{\partial y}$

$+ \delta^2\left(\delta^2\frac{\partial^3 \psi}{\partial x^3} + \frac{\partial^3 \psi}{\partial y^2 \partial x}\right) - \frac{\delta^2}{\gamma^2}\left(\delta^4\frac{\partial^5 \psi}{\partial x^5} + 2\delta^2\frac{\partial^5 \psi}{\partial x^3 \partial y^2} + \frac{\partial^5 \psi}{\partial y^4 \partial x}\right)$
$+ \frac{\delta^2}{Da}.\frac{\partial \psi}{\partial x} - \frac{Re}{Fr}\cos[\alpha]$ (13)

The dimensionless parameters that appeared in Eqs. (12) and (13)

are defined as Re $= \frac{c\rho d_1}{\mu}$ the Reynolds number, $\delta = \frac{d_1}{\lambda}$ the Wave number, $H_a = B_o d_1\sqrt{\frac{\sigma}{\mu}}$ the Hartmann number, $\gamma = d_1\sqrt{\frac{\mu}{\eta}}$ the couple stress parameter, $Da = \frac{k_o}{d_1^2}$ the Darcy number and Fr $= \frac{c^2}{gd_1}$ the Froude number.

The instantaneous volumetric flow rate in the laboratory frame is given by

$Q = \int_{h_2'}^{h_1'} U(X', Y', t')dY'$ (14)

where h_1' and h_2' are functions of X' and t'
Similarly, the rate of volume flow in the wave frame is obtained as

$q = \int_{h_2'}^{h_1'} u'(x', y')dy'$ (15)

Using the frames transformation into Eqs. (14) and (15), the relation between Q and q can be obtained as

$Q = q + c(h_1' - h_2')$ (16)

The time mean flow over a period T at a fixed position X' is defined as

$Q' = \frac{1}{T}\int_0^T Q dt$ (17)

Using Eq. (16) in Eq. (17) the flow rate Q' has the form

$Q' = \frac{1}{T}\int_0^T q dt + c(h_1' - h_2') = q + cd_1 + cd_2$

$+ 2cx\lambda \tan \alpha + ca_1\cos(2\pi x) + ca_2\cos(2\pi x + \phi)$ (18)

Note that $h_1(x)$ and $h_2(x)$ represent the dimensionless form of the peristaltic channel walls given by the equations(10)and(11) of the form

$h_1(x) = 1 + kx + a\cos(2\pi x)$ (19)

$h_2(x) = -d - kx - b\cos(2\pi x + \phi)$ (20)

where $a = \frac{a_1}{d_1}, b = \frac{a_2}{d_1}, d = \frac{d_2}{d_1}, k = \left(\frac{\lambda \tan \alpha}{d_1}\right)$ is called the non-uniform parameter of the channel.
The non-dimensional form of Eq. (18) is now given by
$\theta = F + 1 + d + 2kx + a\cos(2\pi x) + b\cos(2\pi x + \phi)$ (21)
where $\theta = \frac{Q'}{cd_1}$ and F $= \frac{q}{cd_1}$ has the expression in the form

$F = \int_{h_2}^{h_1}\frac{\partial \psi}{\partial y} dy = \psi(h_1) - \psi(h_2)$ (22)

Under the assumption of long wave length approximation ($\delta \ll 1$) and low Reynolds number, (cf. shapiro et al.[7]) eliminating pressure term using cross differentiation from the dimensionless Eqs. (12) and (13) one can write in a single differential equation in terms of stream function ψ as

$\frac{\partial^6 \psi}{\partial y^6}$

The boundary conditions in terms of the stream function ψ (x ,y) in the wave frame can be written as(cf. Shit et al.[9])

$\frac{\partial \psi}{\partial y} + \beta\frac{\partial^2 \psi}{\partial y^2} = -1 \quad on \ y = h_1$

$\frac{\partial \psi}{\partial y} + \beta\frac{\partial^2 \psi}{\partial y^2} = -1 \quad on \ y = h_2$

$\psi = \frac{F}{2} on \ y = h_1$

$\psi = -\frac{F}{2} on \ y = h_2$ (24)

$\frac{\partial^3 \psi}{\partial y^3} = 0 \ on \ y = h_1 \ and \ y = h_2$

The solution of (23) satisfying the corresponding boundary conditions (24) is

$$\psi = \frac{1}{\gamma} 2\sqrt{Da}\left(-\frac{e^{-a1y}c1}{a3} - \frac{e^{a1y}c2}{a3} + \frac{e^{-a2y}c3}{a4} + \frac{e^{a2y}c4}{a4}\right)$$
$$+ c5 + yc6 \qquad (25)$$

The velocity can be written as:

$$u = \frac{2\sqrt{Da}\left(\frac{a1c1e^{-a1y}}{a3} - \frac{a1c2e^{a1y}}{a3} - \frac{a2c3e^{-a2y}}{a4} + \frac{a2c4e^{a2y}}{a4}\right)}{\gamma}$$
$$+ c6 \qquad (26)$$

Once we determined the stream function ψ, the axial pressure gradient can be obtained as

$$\frac{\partial P}{\partial y} = 0 \qquad (27)$$

$$\frac{\partial P}{\partial x} = \frac{\partial^3 \psi}{\partial y^3} - \frac{1}{\gamma^2}\cdot\frac{\partial^5 \psi}{\partial y^5} - H_a^2\left(\frac{\partial \psi}{\partial y} + 1\right) - \frac{1}{Da}\cdot\frac{\partial \psi}{\partial y}$$
$$+ \frac{Re}{Fr}\sin[\alpha] \qquad (28)$$

The pressure rise per wave length Δp in non-dimensional form is defined by

$$\Delta p = \int_0^1 \frac{\partial P}{\partial x} dx \qquad (29)$$

3. Results and Discussion

The analytical expressions for the axial velocity, pressure gradient, pressure rise and stream function are derived in this section. The numerical results corresponding to the abovementioned analytical expressions have been computed using MATHEMATICA subject to the following data:

$Da = 0.1, 2 \ and \ 6$, $H_a = 0.1, 1.6 \ and \ 1.8, b = 0.4$,
$a = 0.5, \gamma = 2, 2.3 \ and \ 2.8,, d = 1, \beta = 0.1, 0.2 \ and \ 0.5$,
$\phi = \frac{\pi}{4}, \frac{\pi}{3} \ and \ \frac{\pi}{2}$, $F = 1, -4 \ and \ -6$,
$k = 0.2, 0.3 \ and \ 0.6, \alpha = \frac{\pi}{6}, \frac{\pi}{4} \ and \ \frac{\pi}{3}$.
$Fr = 0.05, 0.1 \ and \ 1$, $Re = 0.1, 0.2 \ and \ 0.3$

3.1 Velocity distribution

Figs. 2-7 represent the variation of axial velocity u across the channel for different values of the Hartmann number H_a, couple stress parameter γ , the slip parameter β, the Darcy number Da, phase difference ϕ and the non-uniform parameter k . Fig. 2 shows that the axial velocity decreases in the central region of the channel with increasing Hartmann number H_a, while the axial velocity increases in the boundary of the channel wall. The reason behind this fact is the Lorentz force that arises due to the application of an external magnetic field, which plays a vital role in decelerating the fluid motion. Similarly the axial velocity has reducing effect at the central region of the channel and accelerating effect near the channel walls for increasing couple stress parameter γ as shown in Fig. 3 In this case velocity decreases due to the increase of particle size suspended in the fluid itself and causes flattening of the velocity profiles. In order to satisfy the conservation of mass, the flow rate remains same for any value of these parameters at any cross section of the channel. From Fig. 4 shows that the axial velocity decreases in the central region of the channel with increasing the slip parameter β, while the axial velocity increases near the channel walls.This fact is influenced by the presence of velocity slip at the walls for

which the axial velocity is faster at the peripheral region than in its core region. Therefore the slip effect has also significant impact on the axial velocity. It reduces the friction of force at the wall and propel to fluid flow accurately. From Fig. 5 we observed that the axial velocity also decreases at the central region with increasing the non-uniform parameter k of the channel, while the axial velocity increases in the boundary of the channel wall. It is examined in Fig.6 that by increasing phase difference , the velocity of fluid decreases in the region yϵ[-1.5,-0.3] ,whereas it increases in the rest of region. Fig. 7 we observed that the axial velocity increase at the central region with the increase of the Darcy number Da, while the axial velocity decreases in the boundary of the channel wall.
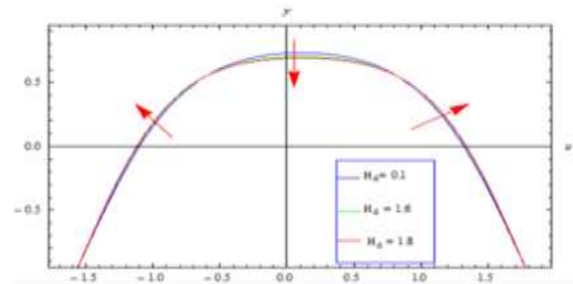

Figure 2: Variation of axial velocity u for different values of H_a with $Da = 0.1, \gamma = 2, a = 0.5, b = 0.4, d = 1, \beta = 0.1$
$Da = 0.1, \gamma = 2, a = 0.5, b = 0.4, d = 1, \beta = 0.1, \phi = \frac{\pi}{4}$,
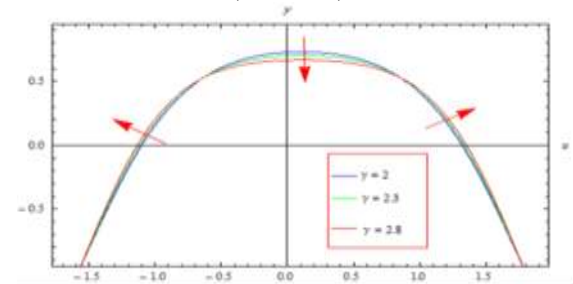$F = 1, k = 0.2, x = 1$

Figure 3: Variation of axial velocity u for different values of γ with $H_a = 0.1, Da = 0.1, a = 0.5, b = 0.4, d = 1$,
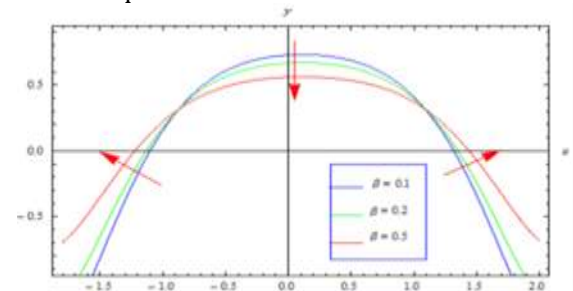$\beta = 0.1, \phi = \frac{\pi}{4}, F = 1, k = 0.2, x = 1$

Figure 4: Variation of axial velocity u for different values of β with $Da = 0.1, H_a = 0.1, a = 0.5, b = 0.4, d = 1$,
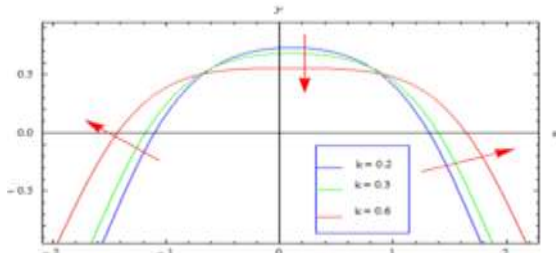$\gamma = 2, \phi = \frac{\pi}{4}, F = 1, k = 0.2, x = 1$

Figure5: Variation of axial velocity u for different values of k with $Da = 0.1, H_a = 0.1$, $\gamma = 2, a = 0.5, b = 0.4,$ $d = 1, \phi = \frac{\pi}{4}, F = 1, \beta = 0.1, x = 1$
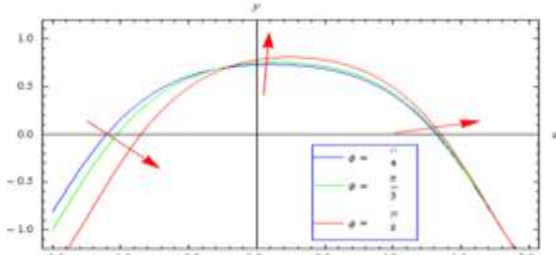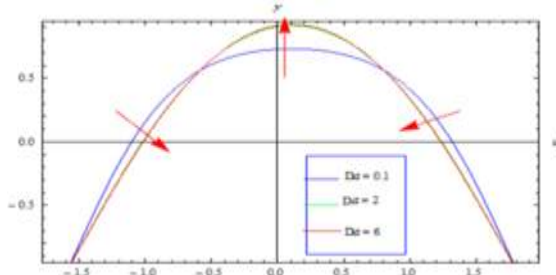

Figure 6: Variation of axial velocity u for different values of $\emptyset$ with $K = 0.2, H_a = 0.1$, $\gamma = 2, a = 0.5, b = 0.4, d = 1,$ $\beta = 0.1$, $F = 1, x = 1, Da = 0.1$

Figure 7: Variation of axial velocity u for different values of Da with $\phi = \frac{\pi}{4}, H_a = 0.1$, $\gamma = 2, a = 0.5, b = 0.4,$ $d = 1, \beta = 0.1, F = 1, k = 0.2, x = 1$

Pumping characteristics 3.2-

Figs. 8-16 illustrate the variation of axial pressure gradient along the Length of the channel in one wave length x $\in[0,1]$. From these figures one can note that through the region $x \in [0.2,0.8]$, i.e. the narrowing part of the channel, flow cannot pass easily. Therefore, it requires more pressure gradient to make it as normal flow. Similarly in the wider part of the channel, i.e. in the region $x \in [0,0.2] \cup [0.8,1]$ fluid can pass easily because of the lower pressure gradient. Fig. 8. we observed that the magnitude of the axial pressure gradient increasing with the increase of the Hartmann number H_a. From this figure. it may point out that when the applied magnetic field is high, then more pressure is needed to pass the same volume of fluid in the narrowing part of the channel. Fig. 9. we observed that the magnitude of the axial pressure gradient increasing with the increase of the Froude number Fr which arises due to the inclination of the channel. However, the trend is reversed in the case of the inclination α of the channel , Darcy number Da, slip parameter β, couple stress parameter γ, phase different ϕ , Reynolds number Re as well as non- uniform parameter k of the channel as shown in Figs.10 - 16 respectively . Therefore, the less pressure is required to fluid flow.

Figs 17-25 depict the variation of pressure rise in function of volumetric flow rate in the wave frame for different values of the Hartmann number H_a , Froude number Fr ,couple stress parameter γ , Reynolds number Re , the slip parameter β , Darcy number Da , phase different ϕ , the non-uniform parameter k and the inclination α of the channel . The whole region is considered into five parts **(i)** peristaltic pumping region where $(\Delta p > 0, F > 0)$. **(ii)** augmented pumping(co-pumping) region where $(\Delta p < 0, F > 0)$. **(iii)** when $(\Delta p > 0, F < 0)$, then it is a retrograde pumping region. **(iv)** There is a co-pumping region where $(\Delta p < 0, F < 0)$. **(v)** $(\Delta p = 0)$ corresponds to the free pumping region. Fig.17 shows that pressure rise Δp increases with increasing Hartmann number H_a. It can be seen from the graph that in a retrograde region $(\Delta p > 0, F < 0)$, the pumping rate decreases in a co-pumping region where $(\Delta p < 0, F < 0)$ with an increase in H_a. Fig.18 shows that pressure rise Δp decreases with increasing Darcy number Da. It is observed the pumping increases in the region of augmented pumping and the co-pumping region $(\Delta p < 0)$. Fig. shows that pressure rise Δp decreases with increasing couple stress parameter γ. It is observed that in a retrograde pumping region $(\Delta p > 0, F < 0)$, the pumping rate increases in a co-pumping region where $(\Delta p < 0)$ with an increase in γ. Fig.20 shows that pressure rise Δp decreases with increasing slip parameter β. It is observed that in a retrograde pumping region $(\Delta p > 0, F < 0)$, the pumping rate increases a co-pumping region where $(\Delta p < 0)$ with an increase in β. Fig.21 shows that pressure rise Δp decreases with increasing non-uniform parameter . It is observed that the pumping rate increases in the co-pumping region $(\Delta p < 0)$ and free pumping region $(\Delta p = 0)$. Fig.22 shows that pressure rise Δp increases with increasing phase different ϕ in a retrograde pumping region. It is observed that the pumping rate decreases in the co-pumping region $(\Delta p < 0)$ with an increase in the phase different ϕ. It is observed from Fig. 23 that an increase in Froude number Fr results in a decrease in retrograde pumping rate $(\Delta p > 0, F < 0)$ and also a decrease in the pressure rise. From Fig. 24 we observed that an increase in the inclination α of the channel results in an increase in retrograde pumping rate $(\Delta p > 0, F < 0)$ and also an increase in the pressure rise. It is observed from Fig. 25 that an increase in Reynolds number Re results in an increase in retrograde pumping rate $(\Delta p > 0, F < 0)$ and also an increase in the pressure rise. It is noticed that there is a linear relationship between pressure rise for each wave length and volumetric flow rate.
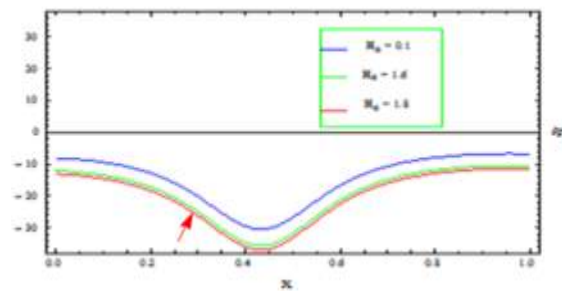

Figure 8: Distribution of pressure gradient $\delta p = \frac{\partial p}{\partial x}$ for different values H_a with $Da = 0.1$, $\gamma = 2, a = 0.5, b = 0.4,$ $d = 1, \beta = 0.1$, $\phi = \frac{\pi}{4}, F = 1, k = 0.2, y = 1$, $Re = 0.1, Fr = 0.05, \alpha = \frac{\pi}{6}$
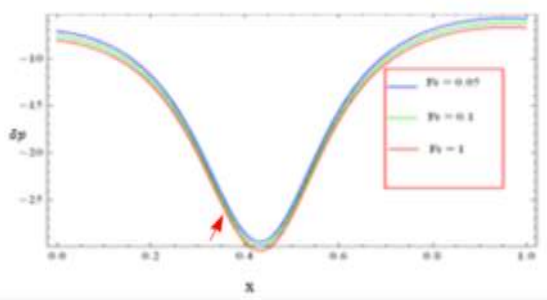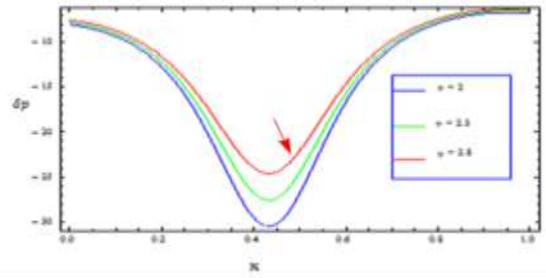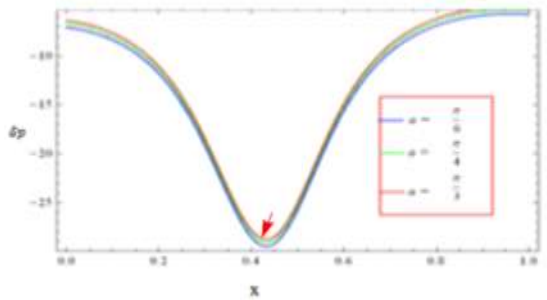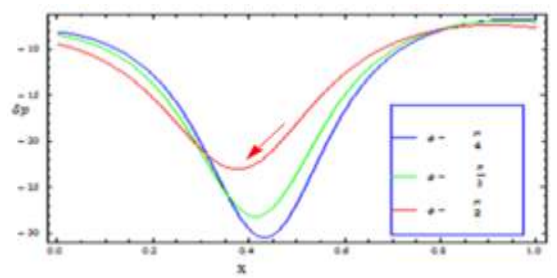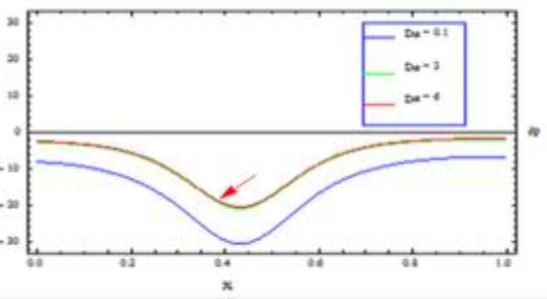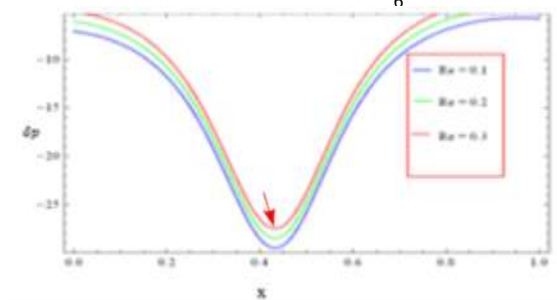
Figure 9: Distribution of pressure gradient $\delta p = \frac{\partial p}{\partial x}$ for different values Fr with $\gamma = 2$, $H_a = 0.1$, $a = 0.5$, $b = 0.4$, $d = 1$, $\beta = 0.1$, $\phi = \frac{\pi}{4}$, $F = 1$, $k = 0.2$, $y = 1$ $Re = 0.1$, D$a = 0.1$, $\alpha = \frac{\pi}{6}$

Figure 10: Distribution of pressure gradient $\delta p = \frac{\partial p}{\partial x}$ for different values α with D$a = 0.1$, $\gamma = 2$, $a = 0.5$, $b = 0.4$, $d = 1$, $\beta = 0.1$, $\phi = \frac{\pi}{4}$, $F = 1$, $k = 0.2$, $y = 1$ $Re = 0.1$, $Fr = 0.05$, $H_a = 0.1$

Figure 11:.Distribution of pressure gradient $\delta p = \frac{\partial p}{\partial x}$ for different values Da with $\gamma = 2$, $H_a = 0.1$, $a = 0.5$, $b = 0.4$, $d = 1$, $\beta = 0.1$, $\phi = \frac{\pi}{4}$, $F = 1$, $k = 0.2$, $y = 1$, $Re = 0.1$, $Fr = 0.05$, $\alpha = \frac{\pi}{6}$
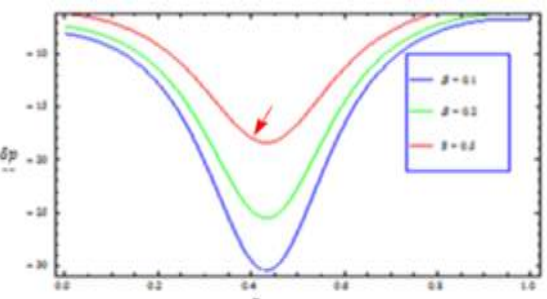

Figure 12:.Distribution of pressure gradient $\delta p = \frac{\partial p}{\partial x}$ for different values of β with D$a = 0.1$, $H_a = 0.1$, $\gamma = 2$, $a = 0.5$, $b = 0.4$, $d = 1$, $\phi = \frac{\pi}{4}$, $F = 1$, $k = 0.2$, $y = 1$, $Re = 0.1$, $Fr = 0.05$, $\alpha = \frac{\pi}{6}$
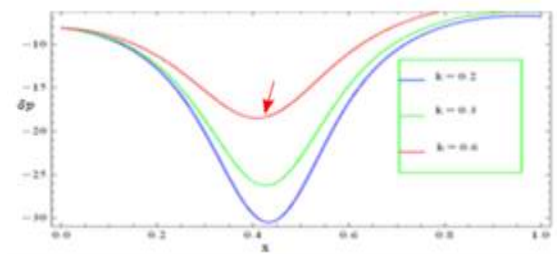

Figure 13:.Distribution of pressure gradient $\delta p = \frac{\partial p}{\partial x}$ for different values γwith D$a = 0.1$, $H_a = 0.1$, $a = 0.5$, $b = 0.4$, $d = 1$, $\beta = 0.1$, $\phi = \frac{\pi}{4}$, $F = 1$, $k = 0.2$, $y = 1$, $Re = 0.1$, $Fr = 0.05$, $\alpha = \frac{\pi}{6}$

Figure 14:.Distribution of pressure gradient $\delta p = \frac{\partial p}{\partial x}$ for differentvalues ϕ with D$a = 0.1$, $H_a = 0.1$, $\gamma = 2$, $a = 0.5$, $b = 0.4$, $d = 1$, $\beta = 0.1$, $F = 1$, $k = 0.2$, $y = 1$, $Re = 0.1$, $Fr = 0.05$, $\alpha = \frac{\pi}{6}$

Figure 15: Distribution of pressure gradient $\delta p = \frac{\partial p}{\partial x}$ for different values of Rewith D$a = 0.1$, $H_a = 0.1$, $a = 0.5$, $b = 0.4$, $d = 1$, $\beta = 0.1$, $\phi = \frac{\pi}{4}$, $F = 1$, $\gamma = 2$, $y = 1$ $\gamma = 2$, $Fr = 0.05$, $\alpha = \frac{\pi}{6}$

Figure 16:.Distribution of pressure gradient $\delta p = \frac{\partial p}{\partial x}$ for different values of k with D$a = 0.1$, $H_a = 0.1$, $a = 0.5$, $b = 0.4$, $d = 1$, $\beta = 0.1$, $\phi = \frac{\pi}{4}$, $F = 1$, $\gamma = 2$, $y = 1$, $Re = 0.1$, $Fr = 0.05$, $\alpha = \frac{\pi}{6}$
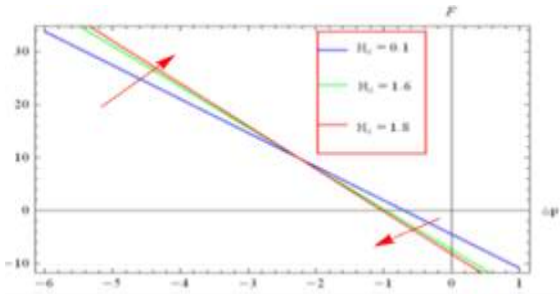
Figure 17: Variation of pressure rise ΔP with F for different values of H_a when $Da = 0.1$, $\gamma = 2$, $a = 0.5$, $b = 0.4$, $d = 1$, $\beta = 0.1$, $\phi = \frac{\pi}{4}$, $k = 0.2$, $y = 1$, $Re = 0.1$, $Fr = 0.05$, $\alpha = \frac{\pi}{6}$
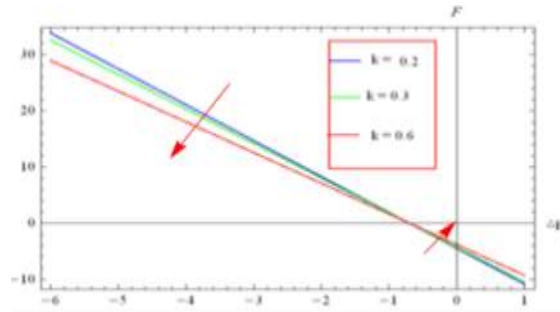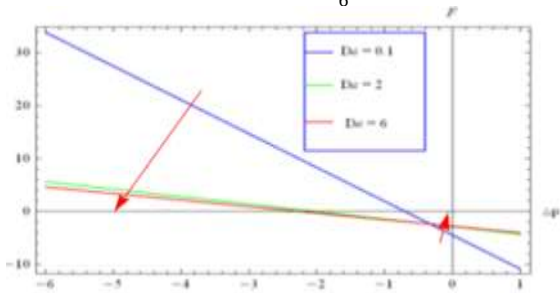

Figure 18: Variation of pressure rise ΔP with F for different values of of Da when $\phi = \frac{\pi}{4}$, $H_a = 0.1$, $a = 0.5$, $b = 0.4$, $d = 1$, $\beta = 0.1$, $\gamma = 2$, $k = 0.2$, $y = 1$, $Re = 0.1$, $Fr = 0.05$, $\alpha = \frac{\pi}{6}$

Figure 19: Variation of pressure rise ΔP with F for different values of γ when $Da = 0.1$, $H_a = 0.1$, $\beta = 0.1$, $a = 0.5$, $b = 0.4$, $d = 1$, $\phi = \frac{\pi}{4}$, $k = 0.2$, $y = 1$, $Re = 0.1$, $Fr = 0.05$, $\alpha = \frac{\pi}{6}$

Figure 20: Variation of pressure rise ΔP with F for different values of β when $Da = 0.1$, $\gamma = 2$, $H_a = 0.1$, $a = 0.5$, $b = 0.4$, $d = 1$, $\phi = \frac{\pi}{4}$, $k = 0.2$, $y = 1$, $Re = 0.1$, $Fr = 0.05$, $\alpha = \frac{\pi}{6}$

Figure 21: Variation of pressure rise ΔP with F for different values of k when $Da = 0.1$, $\gamma = 2$, $H_a = 0.1$, $\phi = \frac{\pi}{4}$, $a = 0.5$, $b = 0.4$, $d = 1$, $\beta = 0.1$, $y = 1$, $Re = 0.1$, $Fr = 0.05$, $\alpha = \frac{\pi}{6}$

Figure 22: Variation of pressure rise ΔP with F for different values of ϕ when $Da = 0.1$, $H_a = 0.1$, $\gamma = 2$, $a = 0.5$, $b = 0.4$, $d = 1$, $\beta = 0.1$, $y = 1$, $k = 0.2$, $Re = 0.1$, $Fr = 0.05$, $\alpha = \frac{\pi}{6}$

Figure 23: Variation of pressure rise ΔP with F for different values of Fr when $Da = 0.1$, $H_a = 0.1$, $\gamma = 2$, $a = 0.5$, $b = 0.4$, $d = 1$, $\beta = 0.1$, $y = 1$, $k = 0.2$, $Re = 0.1$, $\phi = \frac{\pi}{4}$, $\alpha = \frac{\pi}{6}$

Figure 24: Variation of pressure rise ΔP with F for different values of α when $\gamma = 2$, $H_a = 0.1$, $\phi = \frac{\pi}{4}$, $a = 0.5$, $b = 0.4$, $d = 1$, $\beta = 0.1$, $k = 0.2$, $y = 1$, $Re = 0.1$, $Fr = 0.05$, $Da = 0.1$

Paper ID: ART20179754   DOI: 10.21275/ART20179754   13
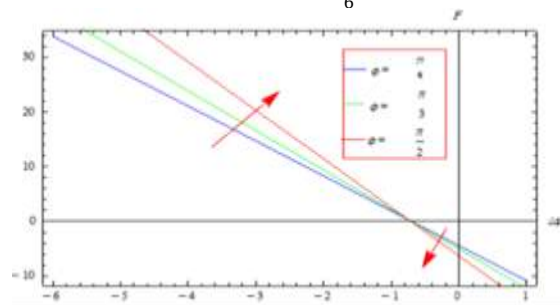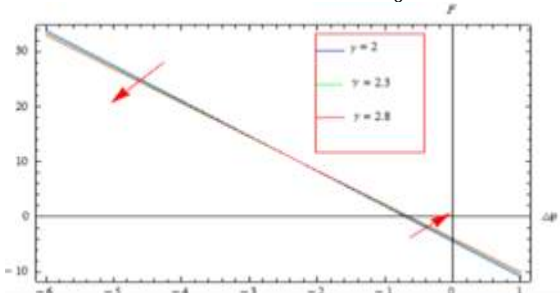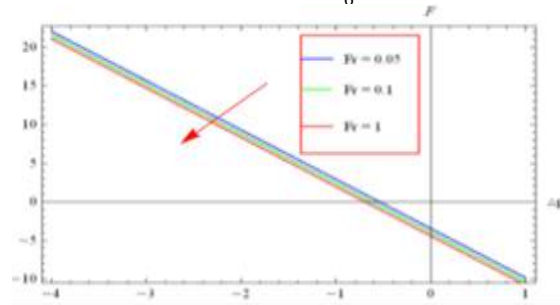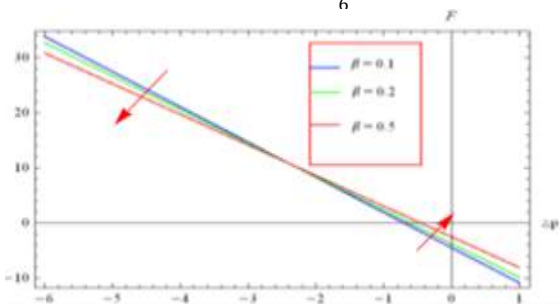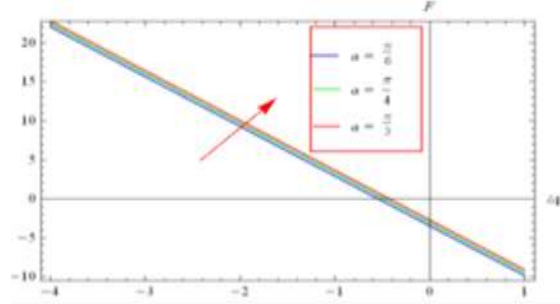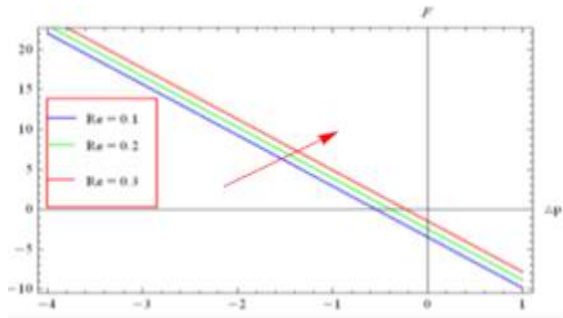
Figure 25: Variation of pressure rise ΔP with F for different values of Re when $Da = 0.1, H_a = 0.1, \gamma = 2, a = 0.5, b = 0.4, d = 1, \beta = 0.1, \phi = \frac{\pi}{4}, y = 1, k = 0.2, Fr = 0.05, \alpha = \frac{\pi}{6}$

Trapping phenomena3.3-

It is known that the phenomenon of trapping is the formation of circulating bolus of the fluid is a region of closed stream lines that move with the wave speed in the wave frame. Owing to the trapping phenomenon, there will exist stagnation points, where both the velocity components of the fluid vanish in the wave frame. It is more necessary to study the stream lines pattern , because of the fact that the difference between the values of the stream function at any two points is used to calculate the flux of fluid or volumetric flow rate through a line connecting the two points. It is observed from Figs.26-30 that the bolus formation takes place on both sides of the central line of the channel in the expanded region. As the magnetic field strength increases the size of the trapped bolus decreases and vanishes in the presence of sufficiently strong magnetic field. Figs. 26(a, b, c) give the variation of stream lines with the variation of the Hartmann number H_a. We have observed that as the Hartmann number increases the bolus size decreases. Figs. 27(a, b, c) give the variation of stream lines with the variation of the Darcy number Da. We have observed that as the Darcy number Da increases the bolus size increase. Figs. 28 (a, b, c) We have observed that as the couple stress parameter γ increases the bolus size decreases and disappears at $\gamma = 2.8$. The effects of slip parameter on the distribution of stream lines are shown in Figs.29(a, b, c) The slip parameter also reduces the formation of trapped bolus. We observed that increase of the slip parameter β the trapped bolus decreases in size and transported and disappears in the downstream direction. The phenomenon of reducing bolus size may help to prevent possible damage of red cells and other constituents. Figs.30.(a, b, c) illustrate the Variation of stream lines with the non-uniformity k of the asymmetric channel. We observed that as the non-uniform parameter k increases the trapped bolus also increases in size and transported in the downstream direction.These figures indicate that in the wider part of the channel, the flow is pulled by the wall, whereas in the a narrow part . the fluid is pushed away from the wall.
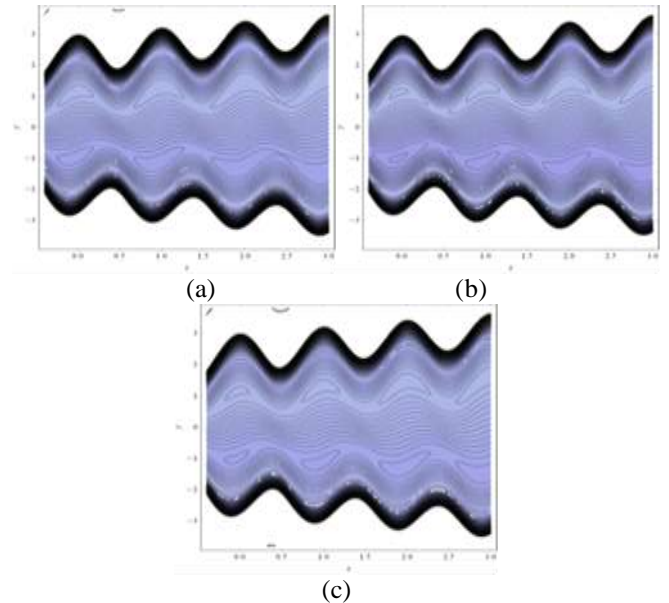

(a)

(b)

(c)

Figure 26: Streamlines (ψ) pattern for $(a)H_a = 0.1, (b)H_a = 1.6, (c)H_a = 1.8$ with $Da = 0.1, \gamma = 2, a = 0.5, b = 0.4, d = 1, \beta = 0.1, \phi = \frac{\pi}{4}, F = 1, k = 0.2$
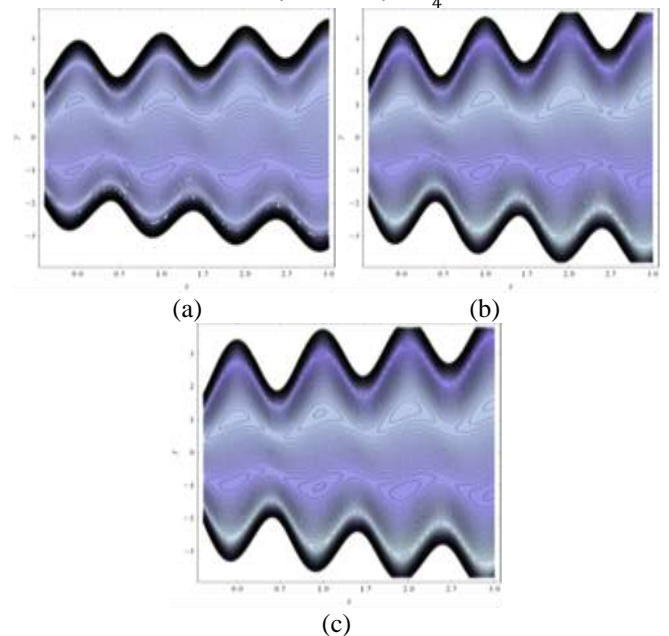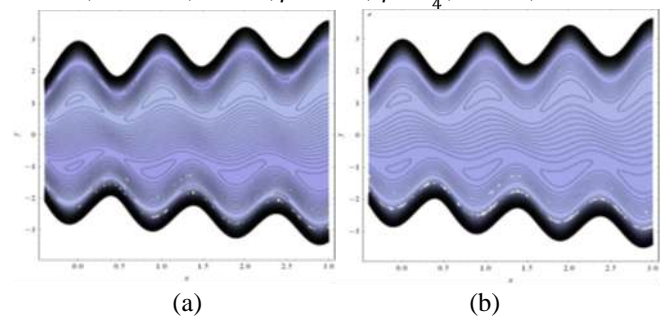

(a)

(b)

(c)

Figure 27: Streamlines (ψ) pattern for $(a)Da = 0.1, (b)Da = 2, (c)Da = 6$ with $H_a = 0.1, \gamma = 2, a = 0.5, b = 0.4, d = 1, \beta = 0.1, \phi = \frac{\pi}{4}, F = 1, k = 0.2$
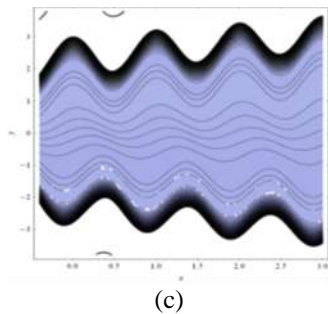

(a)

(b)

(c)

Figure 28: Streamlines (ψ) pattern for$(a)\gamma = 2, (b)\gamma = 2.3$, $(c)\gamma = 2.8$ with$H_a = 0.1$, $Da = 0.1$, $a = 0.5$, $b = 0.4, d = 1$, $\beta = 0.1, \phi = \dfrac{\pi}{4}, F = 1, k = 0.2$
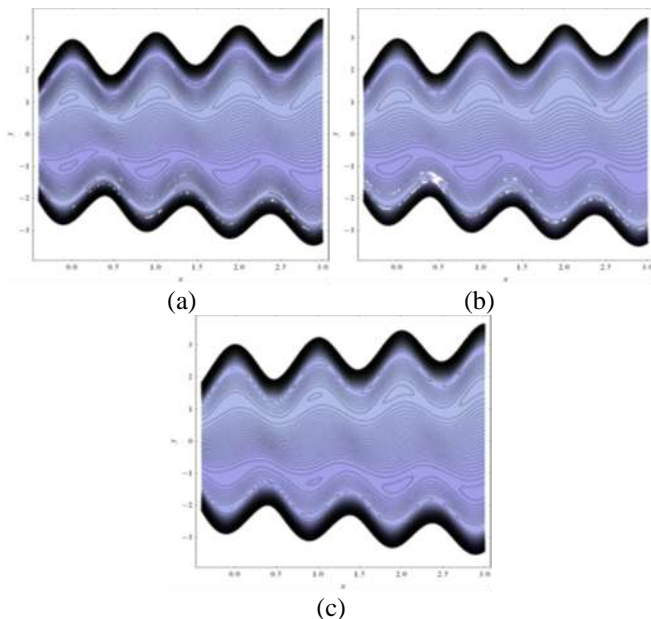

(a)   (b)

(c)

Figure 29: Streamlines (ψ) pattern for$(a)\beta = 0.1, (b)\beta = 0.2, (c)\beta = 0.5$ with$H_a = 0.1, \gamma = 2, a = 0.5$, $b = 0.4$, $d = 1, Da = 0.1$, $\phi = \dfrac{\pi}{4}, F = 1, k = 0.2$
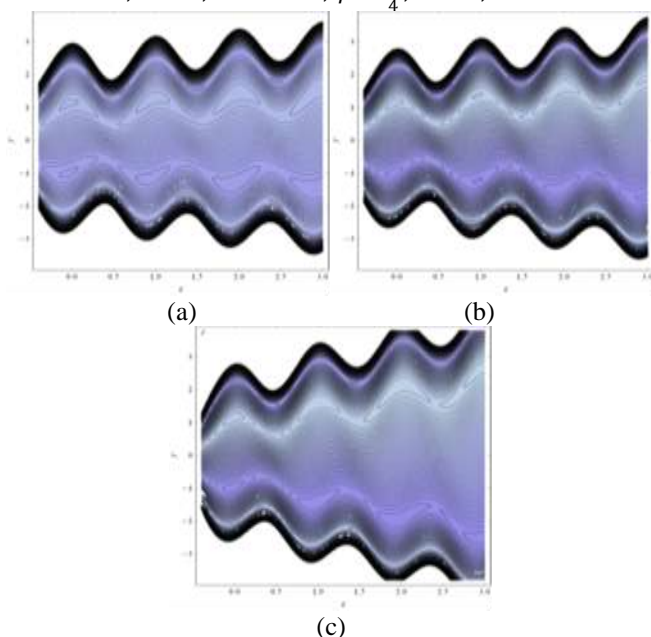

(a)   (b)

(c)

Figure 30: Streamlines (ψ) pattern for$(a)K = 0.2, (b)K = 0.3, (c)K = 0.6$ with$H_a = 0.1, \gamma = 2, a = 0.5, b = 0.4$, $d = 1$, $\beta = 0.1, \phi = \dfrac{\pi}{4}, F = 1, Da = 0.1$

4. Conclusions

In this paper, we have theoretically studied the effects of slip velocity in a peristaltic transport of physiological fluids represented by non-Newtonian fluid model passing through an inclined asymmetric and non-uniform channel with porous medium under the long wave length and low Reynolds number assumptions . In this investigation, special emphasis has been paid to study such as velocity distribution, the pumping characteristic and the trapping phenomena on the basis of a simple analytical solution.

1) The axial velocity(u) at the central region decreases with the increasing values of the Hartmann number(H_a), couple stress parameter (γ) , the slip parameter(β) and non-uniform parameter(k) of the channel , whereas it increases in the boundary of the channel wall.

2) The axial velocity(u) at the central region increases with the increasing values of the Darcy number (Da) , whereas it decreases in the boundary of the channel wall .

3) The axial pressure gradient ($\dfrac{\partial P}{\partial x}$)increases with the increase of Hartmann number(H_a) , Froude number (Fr)whereas it decreases with the increasing values of the inclination(α) of the channel , Darcy number (Da) ,slip parameter(β) ,couple stress parameter (γ), phase difference (ϕ)and Reynolds number(Re) as well as non-uniform parameter (k)of the channel.

4) There is a linear relationship between pressure rise for each wave length and volumetric flow rate

5) The pressure rise increases in retrograde pumping with the increasing valuesH_a , ϕ,α and Re whereasit decreases with the increasing values D_a,γ , β , k and Fr .

6) It may interesting to note that the trapped bolus can be eliminated with the increasing of values couple stress parameter(γ) and the application of strong magnetic field . The role of slip velocity (β)has a reducing effect on the bolus size. whereas it increases the bolus size with the increasing values of the Darcy number (Da) and the non-uniform parameter (k)of the channel.

References

[1] N.Sh. Akbar.,T. Hayat,S. Nadeem,S.Obaidat, (2012) "Peristaltic flow of a Williamson fluid in an inclined asymmetric channel with partial slip and heat transfer", Int.J.Heat Mass Transf.55, 1855-1862.

[2] N.Ali,T. Hayat, (2008) "Peristaltic flow of a micropolar fluid in an asymmetric channel", Comput. Math. Applic .55, 589–608.

[3] M.Kothandapani,S.Srinivas,   (2008)" Non-linear peristaltic transport of a Newtonian fluid in an inclined asymmetric channel through a porous medium", Physics Letters A 372, 1265-1276.

[4] Kh. S.Mekheimer, (2008) "Effect of induced magnetic field on peristaltic flow of a couple stress fluid", Physics Letters A 372, 4271-4278.

[5] M.Mishra,A. R. Rao, (2003) "Peristaltic transport of a Newtonian fluid in an asymmetric channel", J. Appl. Math. Phys. 54 ,532-550 .

[6] K.Ramesh, (2016) "Influence of heat and mass transfer on peristaltic flow of a couple stress fluid through porous medium in the presence of inclined magnetic

field in an inclined asymmetric channel",Jour .Mol. Liq. 2 1 9, 256-271.

[7] A.H.Shapiro,M.Y.Jaffrin,S.L.Weinberg, (1969) " Peristaltic pumping with long wavelengths at low Reynolds number", J. Fluid Mech. 37 (4) ,799-825 .

[8] G.C.Shit,N.K.Ranjit, (2016) "Role of slip velocity on peristaltic transport of couple stress fluid through an asymmetric non-uniform channel: Application to digestive system", J. Mol. Liq . 221 ,305-315.

[9] G.C.Shit, M.Roy, (2014) "Hydromagnetic effect on inclined peristaltic flow of a couple stress fluid", Alex. Eng. Jour . 53 , 949-958.

[10] S.Srinivas , V.Pushparaj, (2008) " Non- linear peristaltic transport in an inclined asymmetric channel", commun. Nonlinear sci. Numer. Simul. l3 ,1782-1795.

[11] V.K.Stokes,(1966) " Couple stress in fluid", Phys. Fluid 9 1709-1715 .

Author Profile

Ahmad M. Abdulhadi I received the B.S and MS.c degree from Baghdad University College of Science-dept. of Mathematics 1988. The Ph.D from Pune Univeristy-India in 2000. He is professor in Mathematics since 2012. Now,working in college of Science-Department of Mathematics.

HanaaAbdulhussain received the B.S degrees in Mathematics from University Baghdad in 2008. In 2009 she was appointed as employee in University Wasit. She is currently studying for a master's degree in applied mathematics in University Baghdad